3rd URSI AT-AP-RASC, Gran Canaria, 29 May – 3 June 2022

Wideband Four-Element MIMO Diversity Antenna using Artificial Transmission Line and Cylindrical Dielectric Resonator for Wireless Applications

Mohammad Ameen* (1) and Raghvendra Kumar Chaudhary(2)
Department of Electronics Engineering, Indian Institute of Technology (Indian School of Mines), Dhanbad-826004, India
(1)mohammadmn61@gmail.com and (2)raghvendra.chaudhary@gmail.com

Abstract

In this work, a new approach is utilized to design a compact Multiple-Input-Multiple-Output (MIMO) antenna by combining the composite right/left-handed (CRLH) transmission line (TL) and cylindrical-shaped dielectric resonator (DR) for the first time. A high level of antenna compactness is achieved due to the loading of the cylindrical-shaped DR above the CRLH-TL. The proposed antenna design starts with a narrowband CRLH-TL antenna, and for further compactness and circular polarization radiation, a cylindrical shaped DR is loaded above the CRLH-TL and converted into a four-element MIMO antenna. The antenna provides wider bandwidth from 2.61–9.40 GHz (113%), isolation better than 17 dB, ARBW of 16.52%, and maximum gain of 3.78 dBi for the complete wideband range.

1. Introduction

The current wireless technologies are focusing on antenna miniaturization with better radiation performance. By utilizing the CRLH-TL based technique can easily achieve antenna miniaturization [1]. Recently, DR [2] based antennas explained in the literature provide higher radiation efficiency with larger antenna volume. Hence the existing DR based antennas are not suitable for modern application systems such as mid-band 5G antenna systems. The combination of CRLH-TL and DR can provide antenna miniaturization and wider bandwidth. Also, for the current applications, MIMO technology is very important due to the requirement high data transmission rate [3].

Several DR based MIMO antennas are explained in the literature. It mainly uses the rectangular-shaped DR for 4G-LTE application [2], hybrid technique for wideband performance [4], three-port MIMO DR antenna for X-band applications [5], six-port MIMO antenna for spatial, polarisation, and angle diversity performance [6]. Multilayer DR based antenna uses frequency selective surfaces for wideband performance [7], pattern diversity due to the back-to-back placement of cylindrical DR elements [8], hemispherical DRA for higher antenna isolation [9], and A-shaped DR for wider bandwidth [10]. Hence due to larger antenna dimensions, the above - explained antennas are unsuitable for modern applications.

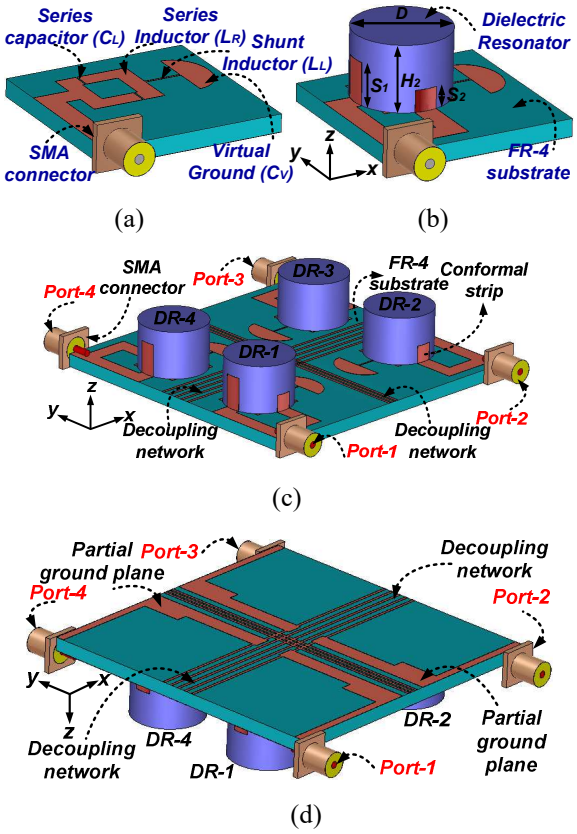

Figure 1. Proposed antenna design. (a) Narrowband CRLH-TL antenna (stage-1), (b) CRLH-TL antenna loaded with cylindrical DR (stage-2), (c) Front view of the MIMO antenna (stage-3), and (d) Back view of MIMO antenna.

This paper proposes a compact four-element wideband MIMO antenna for mid-band 5G and C-band applications. The antenna miniaturization and wideband responses obtained are due to the novel combination of the CRLH-TL and cylindrical shaped DR. According to the author's best of knowledge, this type of CRLH-TL and cylindrical DR based MIMO antenna for wideband application is explaining the first time in literature.

2. Proposed Antenna Geometry and Design

Figure 1(a)–(c) shows the 3D view of the intended four-port MIMO antenna with various stages (stages-1 to stage-3). Firstly, a narrowband MTM antenna is designed as

Table 1: Comparison of the Proposed MTM-DR Loaded MIMO Antenna with Existing DR Loaded MIMO Antennas

Ref. No.	Freq. in GHz	No: of Ports	Dielectric Resonator Shape used	Complete Antenna Size (mm^3)	*ka* value	BW (%)	E-to-E (mm)	Min. Isol. (dB)	Features			
									Wide-band	Com-pact Size	CP Rad.	Via Process
[2]	2.6	2	Rectangular shape	70 × 70 × 11.6	2.69	25	–	20	✓	✕	✕	✓
[4]	4.22	2	Rectangular shape	350 × 350 × 26.1	21.86	38.5	40	28	✓	✕	✓	✓
[5]	9.48	3	Rectangular shape	56.6 × 56.6 × 14	7.94	~ 10	–	20	✕	✕	✕	✓
[6]	2.65	6	Rectangular Shape	100 × 80 × 13.56	3.55	5.24	–	12	✕	✕	✕	✓
[7]	5.25	4	Cylindrical shape	112 × 112 × 33.2	8.70	3.80	14	22	✕	✕	✕	✕
[8]	5.7	4	Cylindrical shape	30 × 30 × 13.6	2.53	10.5	–	18	✕	✓	✕	✕
[9]	5.0	4	Hemispherical	140 × 45 × 8.29	7.69	7.10	15	20	✕	✕	✕	✕
[10]	4.62	2	A-shape	115 × 70 × 21.10	6.50	59.7	21.4	15	✓	✕	✕	✕
This Work	**2.80**	**4**	**Cylindrical shape**	**55 × 55 × 11.4**	**2.27**	**113**	**5**	**17**	✓	✓	✓	✕

Note: Ant.: Antenna, Freq.: Frequency, BW: Bandwidth, E-to-E: End to end distance from one antenna to another antenna, Min. Isol.: Minimum Isolation, Rad.: Radiation, Pro.: Process. (✓ indicates "Yes" and ✕ indicates "No")

shown in Figure. 1(a). The loading of cylindrical-shaped DR above the CRLH-TL antenna is illustrated in Figure. 1(b) provides a wider bandwidth. Finally, a four-port cylindrical DR loaded MIMO antenna configuration is designed, and multiple reflector strips are inserted between the antenna elements as a decoupling network [3], as shown in Figure. 1(c) and (d), respectively. The antenna is designed on FR-4 epoxy substrate (H_1 = 2.4 mm, ε_r = 4.4, and tan δ = 0.02) and alumina DR (H_2 = 9 mm, ε_r = 9.8 and tan δ = 0.001). The $|S_{11}|$ responses corresponding to design stage-1 to stage-3 is depicted in Figure. 2.

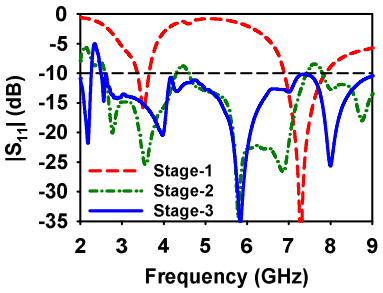

Figure. 2. Input reflection coefficient ($|S_{11}|$) responses for various design stages mentioned in Figure 1(a)–(c).

2.1 Design of CRLH-TL based Single Antenna

Figure. 1(a) depicts the 3D view, and Figure. 3(a)–(c) depicts the schematic view of upper, side and bottom view of the narrowband CRLH-TL antenna mentioned in Figure 1(a) and (b). Figure 3(d) shows the equivalent circuit of the antenna depicted in Figure. 1(a) and (b). The final optimized antenna dimensions of are L = 25, L_f = 18, L_1 = 10, L_2 = 5, L_3 = 11.5, L_4 = 19.5, L_5 = 4, L_L = 5, L_V = 10, L_{R1} = 6.9, L_{R3} = 10, W = 25, W_f = 3, W_g = 20, W_1 = 3, W_2 = 5, W_L = 0.3, C_{L2} = 0.2, and R_V = 4 (All dimensions are in mm).

2.2 Design of DR Loaded CRLH-TL Antenna

Figure. 1(c) and 1(d) depict the 3-D geometry of the CDR loaded CRLH-TL antenna with DR diameter D = 13 mm and height H_2 = 9 mm. From stage-2 of Figure. 2, it is

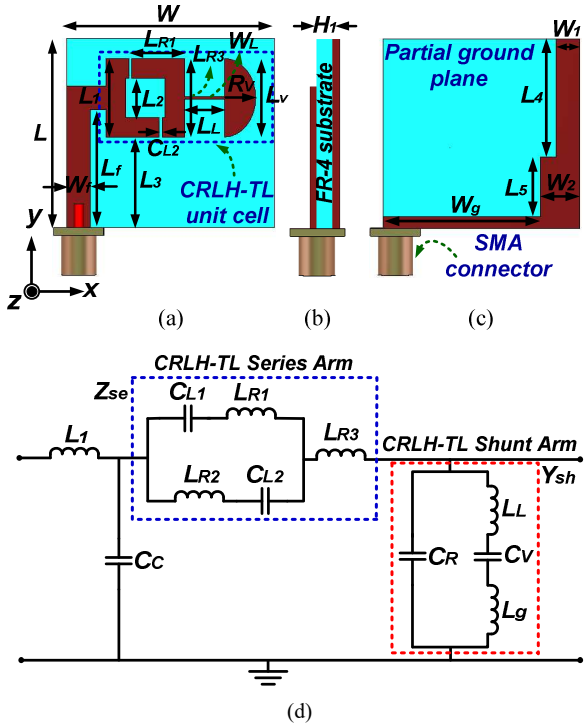

Figure 3. Single element antenna design. (a) Top view, (b) side view, (c) Bottom view, and (d) Equivalent circuit diagram.

noticed that the antenna resonance shifted from 3.53 to 2.6 GHz by cylindrical DR loading. Figure. 4 (a) and (b) shows the parametric studies on $|S_{11}|$ and AR responses by changing the dimension of conformal strips S_1 and S_2. Due to cylindrical DR loading, wider $|S_{11}|$ response is obtained, and conformal strips dimension will control the CP radiation. From Figure. 4(a), there is no involvement in the $|S_{11}|$ responses by varying conformal strips. From Figure. 4(b), it is clearly understood that the best AR performance from 6.02–6.98 GHz 14.76% is noticed at S_1 = 6 mm, S_2 = 3 mm. In Figure. 5(a) to (d), the E-field vector at 6.5 GHz sequentially rotates in the anti-clockwise direction, confirming that the sense of polarization is RHCP.

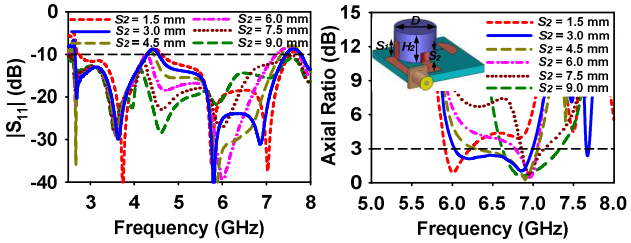

(a) (b)

Figure 4. Parametric studies by by varying the conformal strip S_2 from 1.5 mm to 9 mm by keeping S_1 = 6 mm. (a) $|S_{11}|$ plots, and (b) AR plots.

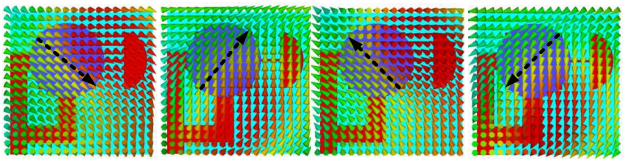

(a) (b) (c) (d)

Figure 5. E-field distributions of the single antenna at 6.5 GHz. (a) $\varphi = 0^0$, (b) $\varphi = 90^0$, (c) $\varphi = 180^0$, and (d) $\varphi = 270^0$.

2.3 Design of Four-port DR Loaded MIMO Antenna with Enhanced Isolation

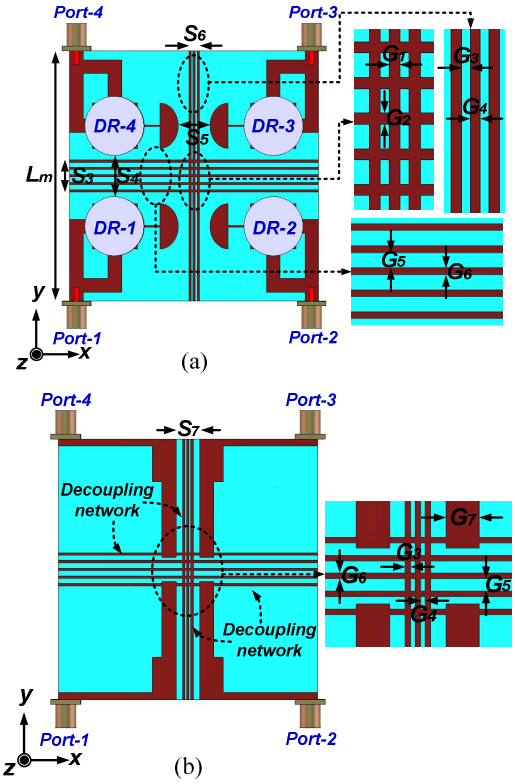

Figure 6. Schematic 2D view of the projected four-element MIMO antenna. (a) Top view and (b) Back view

Figure. 1(c) and 1(d) show the 3D conceptual view of the four-port wideband MIMO antenna configuration. Figure 6(a) and 6(b) shows the schematic front and back view of the four-port MIMO antenna configuration for better understanding. The antenna elements are tightly packed above the substrate with an inter-element spacing S_7 = 5 mm between the individual antenna elements for obtaining antenna compactness. The presented antenna speciality is that loading multiple numbers of reflector strips is arranged in parallel and placed between the individual cylindrical DR loaded antenna can improve antenna isolation [3]. Also, for the MIMO antenna common ground plane, all the antenna grounds are connected. The final antenna dimensions are L_m = 55, S_3 = 6.9, S_4 = 9, S_5 = 7, S_6 = 2.3, G_3 = 0.4, $G_1 = G_2 = G_4 = G_6$ = 0.5, G_5 = 1.1, and G_7 = 3 (All dimensions are in mm).

3. Measurement Results and Discussions

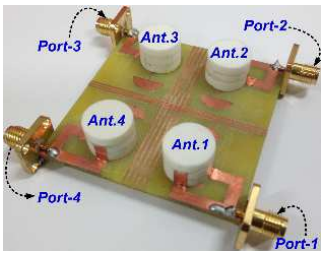

Figure 7. Photograph of the fabricated MIMO antenna.

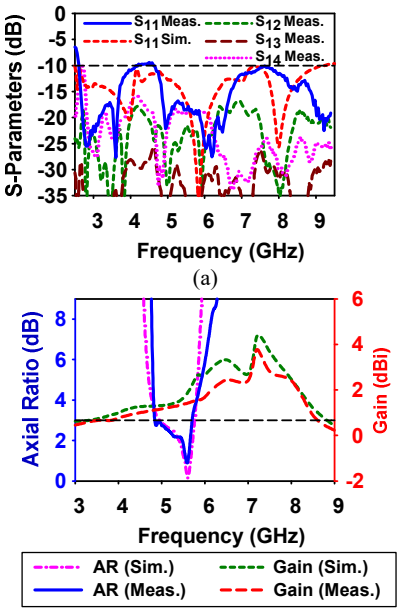

Figure 8. Simulated and measured results. (a) Scattering parameters, and (b) Gain and AR response.

As shown in Figure. 7, the final antenna is fabricated. The antenna shows a simulated $|S_{11}|$ bandwidths of 2.61–9.40 GHz (113.07%) as shown in Figure. 8(a). The isolation between all the individual antenna elements is more than 17 dB for the complete wideband range. The MIMO antenna shows a measured axial ratio bandwidth of 16.52% (4.83–5.7 GHz), measured gain greater than 0.23 dBi with a maximum gain value of 3.78 dBi at 7.2 GHz as shown in Figure. 8(b). The measured radiation patterns for port-1 and Port-2 at 5.5 GHz are depicted in Figure. 9(a) and (b). It is observed that for port-1 RHCP radiation is observed in $+z$ direction and LHCP radiation towards $-z$ direction and vice-versa for the case of port-2.

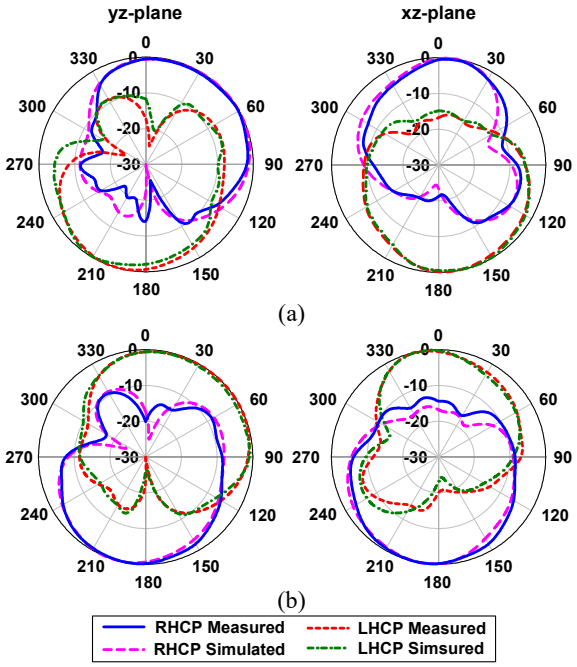

Figure 9. Measured and simulated radiation patterns at 5.5 GHz. (a) Port-1, and (b) Port-2.

3.1 MIMO Antenna Diversity Performance

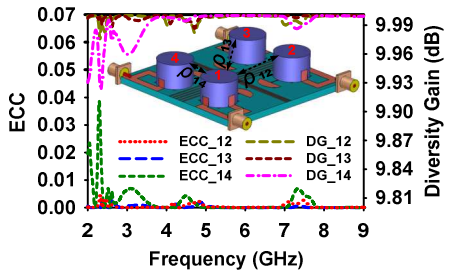

Figure 10. Proposed four-port MIMO antenna ECC and diversity gain.

The envelope correlation coefficient (ECC) and diversity gain responses are presented in Figure. 10 to analyze the performance behavior of the four-port MIMO antenna. For the greatest MIMO antenna performance, the typical value of ECC (ρ_{ij}) is less than 0.05 [3]. For the whole band, the ECC value of the intended Four-port antenna is smaller than 0.02. The fact that the diversity gain is almost near to 10 validates the excellent MIMO antenna performance.

4. Conclusion

This paper presents a unique technique of achieving wideband characteristics with compactness for the four-port MIMO antenna. An array of reflectors based on rectangular strips has been implemented to improve the isolation among the individual antenna elements in the MIMO antenna system. The MIMO antenna provides a wider bandwidth of 113.07% (2.61–9.40) and achieves isolation greater than 17 dB over the entire wideband range. In addition, as compared to similar existing MIMO designs, the antenna maintains a reduced dimension resulting in acceptable gain and ECC values.

5. Acknowledgements

The authors acknowledge the Institution of Electronics and Telecommunication Engineers (IETE), New Delhi, India for financial support by way of PhD Research fellowship.

References

[1] M. Ameen and R. K. Chaudhary, "Metamaterial-based wideband circularly polarised antenna with rotated V-shaped metasurface for small satellite applications," *Electron. Lett.*, **55**, 7, April 2019, pp. 365–366, doi: 10.1049/el.2018.7348.

[2] S. F. Roslan, *et.al*, "An MIMO rectangular dielectric resonator antenna for 4G applications," *IEEE Antennas Wireless Propag. Lett.*, **13**, 2014, pp. 321–324, doi: 10.1109/LAWP.2014.2305696.

[3] S. R. Thummaluru, M. Ameen and R. K. Chaudhary, "Four-Port MIMO cognitive radio system for midband 5G applications," *IEEE Trans. Antennas Propag.*, **67**, 8, August 2019, pp. 5634–5645, doi: 10.1109/TAP.2019.2918476.

[4] J. Iqbal, U. Illahi, M. I. Sulaiman, *et.al*, "Mutual coupling reduction using hybrid technique in wideband circularly polarized MIMO antenna for WiMAX applications," *IEEE Access*, **7**, 2019 pp. 40951–40958, doi: 10.1109/ACCESS.2019.2908001.

[5] A. Abdalrazik, *et.al*, "A three-port MIMO dielectric resonator antenna using decoupled modes," *IEEE Antennas Wireless Propag. Lett.*, **16**, 2017, pp. 3104–3107, 10.1109/LAWP.2017.2763426.

[6] R. Tian, *et.al*, "A compact six-port dielectric resonator antenna array: MIMO channel measurements and performance analysis," *IEEE Trans. Antennas Propag.*, **58**, 4, April 2010, pp. 1369–1379, doi: 10.1109/TAP.2010.2041174.

[7] G. Das, *et.al*, "FSS-based spatially decoupled back-to-back four-port MIMO DRA with multidirectional pattern diversity," *IEEE Antennas Wireless Propag. Lett.*, **18**, 8, August 2019, pp. 1552–1556, doi: 10.1109/LAWP.2019.2922276.

[8] G. Das, *et.al*, "Compact back-to-back DRA-based four-port MIMO antenna system with bi-directional diversity," *Electron. Lett.*, **54**, 14, 2018, pp. 884–886, doi: 10.1049/el.2018.0959.

[9] G. A. Sarkar, *et.al*, "Four element MIMO DRA with high isolation for WLAN applications," *Prog. Electromag. Res. Lett.*, **84**, 2019, pp. 99–106, doi: 10.2528/PIERL19031304.

[10] A. Sharma, *et.al*, "A-shaped wideband dielectric resonator antenna for wireless communication systems and its MIMO implementation," *Int. J. RF Microw. Comput. Aided. Eng.*, **28**, 8, October 2018, e21402, doi: 10.1002/mmce.21402.